HHS Public Access

Author manuscript

J Cell Physiol. Author manuscript; available in PMC 2015 June 07.

Published in final edited form as:

J Cell Physiol. 2011 June ; 226(6): 1702–1712. doi:10.1002/jcp.22501.

High Capacity Na^+/H^+ Exchange Activity in Mineralizing Osteoblasts

Li Liu[1], **Paul H. Schlesinger**[2], **Nicole M. Slack**[1], **Peter A. Friedman**[3], and **Harry C. Blair**[1,*]

[1]Departments of Pathology and Physiology & Cell Biology, Pittsburgh Veteran's Affairs Medical Center, University of Pittsburgh School of Medicine, Pittsburgh, Pennsylvania

[2]Department of Cell Biology and Physiology, School of Medicine, Washington University in St. Louis, St. Louis, Missouri

[3]Department of Pharmacology and Chemical Biology, University of Pittsburgh School of Medicine, Pittsburgh, Pennsylvania

Abstract

Osteoblasts synthesize bone in polarized groups of cells sealed by tight junctions. Large amounts of acid are produced as bone mineral is precipitated. We addressed the mechanism by which cells manage this acid load by measuring intracellular pH (pHi) in non-transformed osteoblasts in response to weak acid or bicarbonate loading. Basal pHi in mineralizing osteoblasts was ~7.3 and decreased by ~ 1.4 units upon replacing extracellular Na^+ with N-methyl-D-glucamine. Loading with 40 mM acetic or propionic acids, in normal extracellular Na^+, caused only mild cytosolic acidification. In contrast, in Na^+-free solutions, weak acids reduced pHi dramatically. After Na^+ reintroduction, pHi recovered rapidly, in keeping with Na^+/H^+exchanger (NHE) activity. Sodium-dependent pHi recovery from weak acid loading was inhibited by amiloride with the Ki consistent with NHEs. NHE1 and NHE6 were expressed strongly, and expression was upregulated highly, by mineralization, in human osteoblasts. Antibody labeling of mouse bone showed NHE1 on basolateral surfaces of all osteoblasts. NHE6 occurred on basolateral surfaces of osteoblasts mainly in areas of mineralization. Conversely, elevated HCO_3^- alkalinized osteoblasts, and pH recovered in medium containing CI-, with or without Na^+, in keeping with Na^+-independent Cl^-/HCO_3^- exchange. The exchanger AE2 also occurred on the basolateral surface of osteoblasts, consistent with Cl^-/HCO_3^- exchange for elimination of metabolic carbonate. Overexpression of NHE6 or knockdown of NHE1 in MG63 human osteosarcoma cells confirmed roles of NHE1 and NHE6 in maintaining pHi. We conclude that in mineralizing osteoblasts, slightly basic basal pHi is maintained, and external acid load is dissipated, by high-capacity Na^+/H^+ exchange via NHE1 and NHE6.

Osteoblasts are among the most metabolically active cells. This is due to synthesis of a collagen matrix and to deposition of hydroxyapatite into that matrix (Blair et al., 2007). Osteoblasts are active in functional units, osteons, of cells connected by gap junctions,

*Correspondence to: Harry C. Blair, Departments of Pathology and of Physiology & Cell Biology, University of Pittsburgh, s705 Scaife Hall, Pittsburgh, PA 15261. hcblair@imap.pitt.edu.

thereby isolating the matrix compartment from the extracellular fluid by tight junctions (Arana-Chavez et al., 1995; Prêle et al., 2003; Blair et al., 2007). The osteon mediates polarized and linear deposition of dense mineral and collagen. Although the process of hydroxyapatite crystal nucleation has been well studied, little information is available regarding the disposition of the metabolic acid and acid evolved during calcium precipitation. This evolved acid must be transported across the tight epithelium-like osteoblast surface layer into the systemic extracellular fluid.

Indirect evidence is consistent with the presence of an actively maintained pH gradient during mineralization (Schartum and Nichols, 1962). More recent findings show that the membrane-bound phosphatase expressed by mineralizing osteoblasts has an alkaline optimal pH (∼8) (Gonçalves et al., 2002). Physiologically, mineralization does not tolerate low pH (acidosis) on the extracellular surface of the osteoblast cells (Brandao-Burch et al., 2005) and therefore acid transport in osteoblasts is not likely to be mediated by large gradientproducing mechanisms, for example, P-type ATP-coupled H^+/K^+ transport or a V-type electrogenic H^+-ATPase. Osteoblasts nonetheless transport substantial acid vectorially during bone formation, and maintain a weak pH gradient, with a higher pH in the matrix than in the general extracellular fluid.

To characterize the mechanism by which mineralizing osteoblasts regulate their pH while extruding H^+ ions, we measured intracellular pH (pHi) in response to weak acids or bicarbonate in non-transformed mineralizing osteoblasts. Primary cultures of human mineralizing osteoblasts were used for most experiments to avoid cell lines that may express transporters different than those in normal mineralizing cells, and to assure that the results reflect processes active in human bone. We show that mineralizing osteoblasts maintain a slightly alkaline cytoplasmic pH. Molecular confirmation of transporter expression was additionally obtained by real-time polymerase chain reactions and by manipulating the expression of NHE1 and NHE6 in osteoblast-like cells. We conclude that acid loads in mineralizing osteoblasts are removed by high-capacity Na^+/H^+ exchange and that metabolic carbonate is eliminated, at least in part, by $\mathrm{Cl}^-/\mathrm{HCO}_3^-$ exchange.

Materials and Methods

Reagents and cell culture

Media and chemicals were from Sigma–Aldrich (St. Louis, MO) unless stated. Normal human osteoblasts and pre-tested media and supplements (Bullet Kits) were from Lonza (Walkersville, MD). The lot of cells we used was from a 6-year-old female. In brief, cells are grown in Dulbecco's modified essential medium with 10% fetal bovine serum, 30 μg/ml ascorbic acid, 30 μg/ml gentamicin, and 15 ng/ml amphotericin-B. To promote osteoblast differentiation, cells were grown to confluence and media supplemented with 200 nM hydrocortisone and 10 mM of 2-glycerol phosphate. Differentiation media were replaced every 3 days; differentiation (Fig. 1A) took 3–5 weeks. In this process, it is crucial to use sufficient medium to avoid acidic conditions or mineralization will not occur (Brandao-Burch et al., 2005). MG63 human osteosarcoma cells and HeLa cervical epithelial cancer cells were from the American Type Culture Collection (Baltimore, MD).

Intracellular pH

The pHi of mineralizing osteoblasts was measured using 2′, 7′-bis-(2-carboxyethyl)-5, 6-carboxyfluorescein (BCECF). Its acetoxymethyl ester derivative (BCECF-AM) is membranepermeant, allowing noninvasive loading of the cells. BCECF-AM, from Molecular Probes (Eugene, OR), was dissolved in dimethyl sulfoxide at 10 mM and stored in a desiccator at –20°C For dye loading, osteoblasts grown on nitric acid-washed 1 × 2 cm, 1 mm thick glass slides were incubated in 140 mM NaCl, 10 mM Hepes, pH 7.4 with 5 μM BCECF-AM for 1 h at 37°C. BCECF-AM is converted to impermeant fluorescent BCECF by cellular esterases. The cells were washed twice with culture medium after loading (Fig. 1B). The fluorescence of BCECF was monitored using an Aminco Bowman Series 2 (AB2) luminescence spectrometer (Thermo Electron, Waltham, MA) with excitation at 500, 455, and 400 nm and a fixed emission of 535 nm. For spectroscopy, glass slides with cells were mounted in a holder to fit in a standard spectrophotometer cuvette with the slide at an angle, 49° to the exciting light, to minimize light scattering into the detector (Okhuma and Poole, 1978). To change media, slides were transferred to a new cuvette mounted in the holder. Calibration of BCECF pH measurement was by the method of Thomas et al. (1979). Calibration solution contained 130 mM KCl, 20 mM NaCl, 5 mM Hepes, and 10 μg/ml H^+–K^+ ionophore nigericin (Teti et al., 1989), to provide rapid intracellular pH equilibration with the bathing solution without compromising cell membrane integrity. Solutions were adjusted to pH 5.0, 5.5, 6.0, 6.5, 7.0, 7.5, and 8.0 using NH_4OH or acetic acid. Excitation scans with fixed emission at 535 nm was performed by placing the BCECF-AM loaded cells in calibration solution at each pH level (Fig. 1C). For real-time pH measurement, standard solution was 140 mM NaCl, 3 mM KCl, 1.5 mM $CaCl_2$, 5 mM Hepes, and 5 mM D-glucose, with substitutions and additions as indicated in Results Section. Hepesbuffered solution was used to minimize contribution of transporters other than the Na^+/H^+ exchanger to pHi regulation. Standard curves relating fluorescence ratios at two-excitation wavelength with background fluorescence subtracted [(500 nm – 400 nm)/(455 nm – 400 nm)] to pHi were from these scans. The standard curve (Fig. 1D) was used to convert the fluorescence ratio to pHi. To determine the BCECF dissociation constant (pK_a), the pH values were plotted as a function of log[(R – RA)/(RB – R) × F455A/F455B], where R is the fluorescence ratio (F500/F455) of the sample, RA is the fluorescence ratio (F500/F455) of the pH 5.0 solution, RB is the fluorescence ratio (F500/F455) of the pH 8.0 solution, F455A is the fluorescence intensity at 455 nm of the pH 5.0 solution, and F455B is the fluorescence intensity at 455 nm of the pH 8.0 solution. The pK_a was estimated from the X-intercept of a linear regression fit.

Mouse bone frozen sections

Procedures were approved by the institutional animal care and use committee. Sixteen-week-old male C57 black mice were injected with calcein intraperitoneally, 1 μg/g animal weight, 4 days and 1 day prior to sacrifice to label mineral deposition. Vertebrae L1– L3 were embedded in gelatin and snap frozen in liquid nitrogen. Sections of 4 μm were cut on a Microm HM 505E cryostat using tape transfer to capture the bone (CryoJane, Instrumedics, St. Louis, MO).

Antibody labeling

Fluorescent antibody localization was performed on sections of mouse bone. Sections were air dried, fixed with cold acetone, and used for antibody labeling as described (Blair et al., 2009). Primary goat anti-NHE6 (anti C-terminal 20-mer peptide; sc-16111), goat anti-NHE1 (anti-C-terminal 20-mer peptide; sc-16097), and goat anti-AE2 (anti-N-terminal 12-mer; sc-46710), and corresponding immunizing peptide antigens, were from Santa Cruz Biotechnology (Santa Cruz, CA). They were applied at 4 μg/ml for 1 h at room temperature, followed by donkey anti-goat Cy3 (Jackson Laboratories, West Grove, PA) for 1 h at room temperature. Fluorescent-labeled proteins were photographed using 1.3 NA40 or 100 oil objectives on a Nikon TE2000 microscope. Images were acquired using a 14 bit 2,048 × 2,048 pixel charge-coupled detector array (Diagnostic Instruments, Sterling Heights, MI). Green channel indicates signal from excitation 450–490 nm, a 510 nm dichroic mirror, and a 520 nm barrier; red signal represents excitation 536-556 nm, a 580 nm dichroic mirror, and a 590 nm barrier.

RNA and quantitative PCR

Total RNA was isolated by oligo dT affinity (RNeasy, Qiagen, Valencia, CA) and cDNA was synthesized using random hexamers and Moloney murine leukemia virus (M-MLV) reverse transcriptase (Superscript III; Invitrogen, Carlsbad, CA). Quantitative PCR was performed with the MX3000P instrument (Stratagene, La Jolla, CA) using SYBR Green to monitor DNA amplification. The reaction was performed in duplicate, in a 25 μl reaction volume containing 12.5 μl of pre-mixed dye, nucleotide triphosphates, buffer, and polymerase (SYBR Green Master Mix, Stratagene), to which 250 nM primers and 1 μl of first strand cDNA were added. After 10 min at 95°C, the mixture was amplified in cycles of 30sec at 95°C, 30 sec at 59°C, and 1 min at 72°C Specificity of PCR products was verified by size with agarose gel electrophoresis and ethidium bromide to visualize products. Primers were: hNHE1, GenBank NM_003047.3, forward: 5′-TCT GCC GTC TCC ACT GTC TCC A-3′, reverse: 5′-CCC TTC AGC TCC TCA TTC ACC A-3′ (422 bp). hNHE6, NM_001042537.1, forward: 5′-TGC CAT AGT GCT GTC CTC CTC AAT-3′, reverse: 5′-AAA GCT GTC ACC ACT CCA GTA GCA-3′ (159 bp); human glyceraldehyde-3-phosphate dehydrogenase (hGAPDH) was used as a control gene for human targets, NM_002046.3, forward: 5′-ACA GTC AGC CGC ATC TTC TT-3′ reverse: 5′-GAC AAG CTT CCC GTT CTC AG-3′ (259 bp). Product abundance relative to the control was calculated assuming linearity of threshold cycle to log (initial copies) as –(Ctcontrol – CtNHEx) (Bustin, 2000).

siRNA, DNA plasmids, and transfection

Knockdown of basal expression levels of NHE1 in MG63 cells was performed using NHE1 siRNA, using scrambled siRNA as a control (Santa Cruz Biotechnology). NHE6 expressing plasmid (NHE6.0) was a gift of Dr. Masao Sakaguchi (University of Hyogo, Japan). The plasmid construct is published (Miyazaki et al., 2001). Control pRcCMV vector for the NHE6 plasmid was from Invitrogen. MG63 cells were grown on glass chips in 60 mm dishes at 80–90% confluence for DNA plasmid transfection, and 30–40% confluence for siRNA transfection. Plasmid DNA of 8 μg or 200 pmol siRNA was transfected into the cells

using Lipofectamine 2000 (Invitrogen). Forty-eight hour after plasmid DNA transfection or 72 h after siRNA transfection, the cells grown on glass were used for intracellular pH measurement. Parallel cultures were collected for RNA isolation.

Statistics

Ranges are standard deviations of three or more measurements unless stated. Comparisons of differences used Student's *t*-test.

Results

Mineralizing human osteoblasts and intracellular pH (pHi) measurement

Mineralizing foci in osteoblast cultures are clearly demonstrated without staining (Fig. 1A); the mineral reflects light and appears dark in transmitted light. pHi was measured by loading the cells with BCECF. To show that acetoxyl cleavage was sufficient for pH determination and to control for factors including autofluorescence that might influence determination, a titration curve was produced as shown in Figure 1B–D. The measured pK_a of 7.087 ±0.056 measured in cultured osteoblasts is near the reported value of 7.0 (Teti et al., 1989), indicating that mineralizing osteoblasts pHi can be evaluated using this method.

Basal pHi of mineralizing osteoblasts

Resting pHi of mineralizing human osteoblasts was 7.35 ± 0.03, close to the physiologic extracellular pH. In contrast, the pHi of non-mineralizing human osteoblasts was 6.62 ± 0.02 and was statistically different ($P < 0.01$), as though a high-capacity proton exporting mechanism was absent (Fig. 2A). As an additional control, pHi in non-skeletal HeLa cells was measured in the same culture conditions and it was similar to that of the non-mineralizing osteoblasts (not shown). This suggested that, prior to mineralization, the osteoblast in culture has poorly developed proton export capacity which is massively upregulated as mineralization begins.

High capacity Na^+/H^+ exchange activity in mineralizing osteoblasts

We compared the response of mineralizing osteoblasts, non-mineralizing osteoblasts and HeLa cells, which do not produce matrix, to a 40 mM propionic acid load (Fig. 2B). Under this large acid challenge, mineralizing osteoblasts displayed only a minor deviation from resting pHi of 0.14 pH units, whereas non-mineralizing osteoblasts exhibited a drop of pHi of 0.62 units and HeLa cells of 0.58 units. The resistance to pH change demonstrates that mineralizing osteoblasts have a distinct transport mechanism that enables them to regulate pHi in response to a large acid load. We further characterized H^+ transport in mineralizing osteoblasts by removing extracellular Na^+ (Fig. 2C). Na^+ removal causes intracellular acidification; with Na^+ reintroduction, recovery from the acidosis occurs, consistent with Na^+/H^+ exchange (Steeves et al., 2001). The initial recovery rate after Na^+ reintroduction reflects Na^+/H^+ exchanger activity (Erdogan et al., 2005), although not necessarily Na^+/H^+ exchange capacity since the exchange activity may be regulated by other factors. Specifically, in mineralizing osteoblasts, replacement of extracellular Na with N-methyl-D-glucamine ($NMDG^+$) decreased osteoblasts pHi by 1.35 ± 0.05 units, with a rate of 0.24 ± 0.01 pH units/min. The half time of acidification was ∼ 105 sec. Following acidification,

pHi did not recover until Na^+ was restored, which induced an extremely rapid recovery, with an initial rate of 5.57 ± 0.02 units/min. The initial pHi recovery rate upon Na^+ reintroduction is much higher than that in non-mineralizing osteoblasts ($P< 0.001$), or when compared to pHi recovery rates of other cell types (Helbig et al., 1988; Erdogan et al., 2005). In non-mineralizing osteoblasts, Na^+ removal caused only a pHi decrease of 0.33 ± 0.01 units, with a rate of 0.05 ± 0.03 pH units/min. The initial recovery rate after Na^+ replacement was only 0.10 ± 0.03 pH units/min. The large difference in cell acidification upon Na^+ removal and recovery after Na^+ replacement between mineralizing and non-mineralizing osteoblasts is indicative of high-capacity Na^+/H^+ exchange in mineralizing osteoblasts.

To characterize Na^+/H^+ exchange activity further, we exposed mineralizing osteoblasts to acid loads in the presence or absence of Na^+. Potassium acetate or potassium propionate, 40 mM, were used, in buffers at pH 7.4. At physiological pH, acetate and propionate are in equilibrium with their non-ionized forms, acetic acid or propionic acid, which diffuses into the cell and causes intracellular acidosis. In the presence of extracellular Na^+, either acetate or propionate acid loading caused only mild cytoplasmic acidification (ΔpHi 0.1 ± 0.02 units; at an initial rate of 0.162 pH unit/min for acetic acid loading; an average pHi drop of 0.15 ± 0.03 units, at a rate of 0.58 ± 0.05 pH unit/min for propionate). This acidification was followed by pHi recovery to the initial resting level at a rate of 0.04 ± 0.02 pH unit/min, in either acetate or propionate. Removal of the acid load caused, as expected, initial alkalinization as the non-ionized acid diffuses out of the cells, followed by a recovery to resting pHi (Fig. 2D, E). The slight difference in acidification rate and magnitude induced by propionate may reflect metabolism of acetic acid or other factors, such as differences in permeability. In striking contrast, when acid loads were applied in the absence of extracellular Na^+, the magnitude of acidification increased, threefold in acetate, 1.6-fold in propionate. Under these conditions, the acidification rate was 7 times higher in acetate and 6.5 times higher in propionate compared to acid loading in the presence of Na^+ (Fig. 2D, E). Further, pHi not only failed to recover but also decreased asymptotically until Na^+ was reintroduced. There was minor variation from culture to culture in minimum pH ∼0.5 pH unit between preparations; the reason for this stochastic variation was unclear. Upon Na^+ replacement, initial pHi recovery rate was 2.88 ±0.12 pH unit/min in acetate, 6.78 ± 0.18 pH unit/min in propionate (Fig. 2F). The difference in pHi changes after acid load with and without extracellular Na^+ is due to high basal Na^+/H^+ exchange activity in mineralizing osteoblasts and may contribute to the higher basal intracellular pH in these cells.

The data in Figure 2D were used to calculate the intracellular buffering power (B) of mineralizing osteoblasts. B is a measure of the cell's ability to resist the changes of pHi. With 40 mM acetate acid load in the presence of Na^+, the apparent B of mineralizing osteoblasts is 220 mM. However, with the same acid load but in the absence of Na^+, the apparent B is 30 mM, which is in the range of B reported in other cell types (Roos and Boron, 1981). This indicates that Na^+/H^+ exchange contributes to the small excursion of pHi in mineralizing osteoblasts in an acid load, which leads to an overestimation of intracellular buffering power.

Amiloride blocks pHi recovery from acid loading

We examined sensitivity of pH recovery from acid loads in the presence of Na^+ to the Na^+/H^+ exchange antagonist amiloride (Fig. 3). The cells were exposed to 40 mM potassium acetate in the presence of 0, 10, 30, and 90 μM amiloride. Figure 3A shows an example of 10 μM amiloride on pHi recovery. Figure 3B shows the pH recovery rate as a function of amiloride concentration, and the same data plotted as fractional inhibition as a function of amiloride concentration (Fig. 3C). The results suggest the presence of high ($IC_{50} \sim 15$ μM) and low (> 100 μM) amiloride sensitive Na^+/H^+ exchange. Amiloride sensitivity in different cell cultures gave similar results (not shown). These data suggest there are two or more Na^+/H^+ exchangers on mineralizing osteoblasts. The IC_{50} of 15 μM is consistent with the amiloride sensitivity of the most commonly expressed Na^+/H^+ exchanger, NHE1 in some cell types (Kulanthaivel et al., 1992; Schwark et al., 1998), although typical IC_{50} of NHE1 is ∼1–5 mM in most contexts. The component that is relatively insensitive might represent NHE6, which is less sensitive to amiloride.

Expression of NHE1 and NHE6 in human mineralizing and non-mineralizing osteoblasts

To determine Na^+/H^+ exchanger isoforms expressed by mineralizing osteoblasts, we used cRNA screening. Although we do not exclude low level expression of other isoforms, we detected only two isoforms, NHE1 and NHE6, at levels significantly above background (not shown). The two significantly expressed isoforms were studied by real-time PCR in human mineralizing and non-mineralizing osteoblasts. In addition to normal human osteoblasts, MG63 human osteosarcoma cells were studied. MG63 cells have features of immature osteoblasts, and do not mineralize in the tissue culture conditions used here. Figure 4A shows that in MG63 cells, NHE1 expression is similar in growing cells and cells treated with osteoblast differentiation medium. In contrast, NHE1 expression in mineralizing human osteoblasts is 5 times higher than that of non-mineralizing osteoblasts. Similar results for NHE6 expression is shown in Figure 4B. NHE6 expression increases threefold in mineralizing normal osteoblasts compared to that in growing, non-mineralizing osteoblasts. In MG63 cells, NHE6 expression was low and did not change with exposure to differentiation medium. These results indicate that both NHE1 and NHE6 expression are upregulated in mineralizing osteoblasts.

Next, we used immune labeling of frozen sections of mouse bone to determine the expression pattern of NHE1 and NHE6 on bone lining and on mineralizing osteoblasts. Figure 4C, D shows fluorescent immune labeling of NHE1 and NHE6 in sections of vertebral mouse bone. The mice were injected with calcein four and one day(s) before sacrifice to label the newly formed mineral to identify where active mineralization was occurring in vivo. Calcein (green fluorescence)-labeled mineralization is shown in the middle row of Figure 4C, D. The bottom row shows the green fluorescence overlaid with the red signal of NHE1 or NHE6. Antibody specific for NHE1 labeled the basolateral (extracellular fluid-exposed) surfaces of all osteoblasts on bone, without correlation with bone mineralization, consistent with its presence in both mineralizing and non-mineralizing cells. In contrast, antibody to NHE6-labeled osteoblasts on bone mainly at sites of mineralization. In addition, NHE6 was present in many bone marrow cells (labeled * in Fig. 4D). Negative controls were performed using blocking peptides to neutralize each primary

antibody and these showed no cell labeling (Fig. 4C, D, second and fourth columns). Figure 4E shows at higher power NHE6 at the basolateral surface of osteoblasts on mineralizing bone. Figure 4E(a) shows, where the arrows indicate, the basolateral surface of bone-lining osteoblasts in phase (grey). In Figure 4E(b), NHE6 staining is seen at exactly the same surface of osteoblasts, at site of active mineralization. Although we cannot exclude intracellular NHE6 signals, when merged with bright field image, NHE6 staining overlay with cell surface of bone-lining osteoblasts (Fig. 4E(c)). Therefore, to the limit of resolution of the method (~200 nm), NHE6 signal colocalizes with the basolateral surface of bone-lining osteoblasts. These data indicate that, although NHE1 is expressed on all bone surfaces, NHE6 is probably important at sites of active mineralization. This is consistent with recent reports that the NHE6 is directed to the cell surface under some conditions (Ohgaki et al., 2008).

Na^+-independent HCO_3^-/Cl^- exchange in mineralizing osteoblasts

Due to the metabolic activity, osteoblasts also produce significant intracellular bicarbonate. To prevent excess intracellular alkalinization, other acid transporting cells typically express anion exchanger (AE) family genes to export HCO_3^-. Figure 5A, B shows that exposure of BCECF-loaded osteoblasts to 40 mM bicarbonate at pH 7.4 resulted in an increase of 0.69 ±0.01 pH unit. Removal of bicarbonate led to a rapid decrease of pHi to resting level with an initial rate of 0.15 ±0.03 pH unit/min, corresponding to HCO_3^- export from the cell (Fig. 5A, black trace). HCO_3^- export was not affected by Na^+ removal (Fig. 5A, grey trace, initial recovery rate: 0.16 ± 0.03 pH unit/min), but inhibited by Cl^- removal (Fig. 5B), consistent with Na^+-independent HCO_3^-/Cl^- exchange (Bronckers et al., 2009). This also excludes the possibility that the Na^+-dependent pH regulation observed in Na^+/H^+ exchange studies is complicated by Na^+-dependent HCO_3^- transport. We examined anion exchangers expressed on osteoblasts; Figure 5C shows immune labeling of AE2 on mouse bone. Its bone surface expression pattern is similar to NHE1; that is, it is expressed on all bone surface, not limited to areas of new bone formation, which are labeled with calcein (left part). AE2 labeling was also neutralized by the specific blocking peptide, which showed no labeling on bone surface (Fig. 5C, right part).

NHE6 overexpression and NHE1 knockdown in MG63 cells

To distinguish the effects of NHE1 and NHE6 on pHi, we used molecular manipulation of NHE1 and NHE6 expression in MG63 cells. Overexpression of NHE6 in MG63 cells leads to a pHi up-shift by an average of 0.34 units (Fig. 6A, B). Upon Na^+ withdrawal, control (vector transfected) MG63 cells exhibited pHi changes similar to that of non-mineralizing normal osteoblasts (Fig. 6A, black trace compared to Fig. 2C, grey trace), with an average pHi decrease of 0.23 units and an average initial pHi recovery rate of 0.11 pH units/min after Na^+ replacement. However, in NHE6-overexpressing MG63 cells, Na^+ withdrawal caused a dramatic decrease in pHi, with an average initial recovery rate of 9.6 pH units/min. These data strongly support that NHE6 contributes to high basal Na^+/H^+ exchange activity and helps maintain an alkaline resting pHi. We next exposed the cells to 40 mM acetic acid load. Under this stimulus, NHE6-expressing and control MG63 exhibited similar pHi changes, except that in control cells, the pHi recovery slowed markedly after an initial fast

recovery, whereas in NHE6-expressing cells the recovery rate was essentially uniform throughout the recovery phase (Fig. 6B). These results are typical of three independent experiments. Figure 6C shows that NHE6 mRNA expression in NHE6-expressing MG63 is 250 times higher than that in control MG63 cells. We next reduced NHE1 in MG63 cells via NHE1 siRNA. Figure 6E demonstrates that NHE1 siRNA transfection decreased NHE1 mRNA expression by 65% compared to that of control MG63 cells. That the knockdown is incomplete is probably due to the technical difficulty in achieving uniform transfection. Figure 6D shows that NHE1 knockdown resulted in a decrease in resting pHi of an average of 0.26 units. When these cells were subjected to a 40 mM acetic acid load, NHE1 knockdown cells demonstrated a marked decrease in recovery rate from acid load of 60% that of the control cells, which is consistent with the role of NHE1 as a housekeeping gene to maintain intracellular pH. Taken together, our data indicate that both NHE1 and NHE6 function to maintain resting pHi. Higher expression levels of NHE1 and NHE6 contribute to alkaline resting pHi.

Discussion

Osteoblasts must transport sufficient acid equivalents to prevent intracellular acidification which would suppress the formation of bone mineral. Precipitation of bone mineral liberates approximately 1.5 moles of H^+ per mole of calcium precipitated (Blair et al., 2007). This acid obviously must be transported across the tight epithelium-like layer of osteoblasts into the systemic extracellular fluid. This large acid flux is similar to that for acid secreting cells such as osteoclasts, renal tubular cells, and gastric parietal cells. In this work, we characterized the mechanism by which osteoblasts export large quantities of acid produced during mineralization. Our findings demonstrate that mineralizing osteoblasts have a remarkably high rate of Na^+/H^+ exchange activity, which is not present in cell before they are competent to sustain mineralization. Accordingly, we find NHE1 is upregulated 5 times and NHE6, an unusual NHE isoform, is upregulated 3 times in mineralizing osteoblasts compared to non-mineralizing osteoblasts. The observed levels of NHE1 and NHE6 exceed those required for normal pHi regulation and reflect an adaption to the mineralization function of osteoblasts, which cannot occur without dissipating a large acid load accumulated in mineralizing osteoblasts.

Although both NHE1 and NHE6 might be exhibiting redundant function their different location suggests that they contribute independently to pHi regulation. In MG63 and non-mineralizing normal osteoblasts, NHE1 expression is 2.3 and 2.7 times higher than NHE6, respectively (data not shown). When these cells were subjected to acid load, the recovery rate usually slow down after an initial faster phase and cannot achieve full recovery (Fig. 2A, thick grey trace; Fig. 6B, black trace). However, in NHE6 transfected MG63 cells and mineralizing normal osteoblasts, the recovery rate did not change and complete recovery was achieved (Fig. 6B, grey trace; Fig. 2A, black trace) after subjected to an acid load. In addition, knocking down NHE1 resulted in a slower initial recovery rate in MG63 cells with an acid load (Fig. 6D). This suggests that NHE1 and NHE6 both contribute to acid extrusion but the two exchangers have distinct turnover rates. NHE6 is found in mineralizing osteoblasts at the basolateral surface, whereas all bone-lining osteoblasts (active or inactive) express NHE1. This suggests a role of NHE6 in mineraliztion-specific regulation, although

the functional significance is not known. This may become clear when the regulation of sodium–hydrogen exchange during bone formation can be studied in more detail.

Na^+/H^+ exchanger (NHE) activity is important for intracellular pH homeostasis in many cells, especially under acidic conditions. The electroneutral Na^+/H^+ exchangers, which export H^+ in exchange for Na^+ moving down its inward concentration gradient, mediate acid extrusion from the cytosol (Orlowski and Grinstein, 2004), thereby protecting cells against cytosolic acidification and maintaining intracellular pH. These exchangers are regulated by multiple factors, typically coordinated by Na^+/H^+ exchange regulatory factors (NHERFs) (Hayashi et al., 2002; Capuano et al., 2007; Cardone et al., 2007; Seidler et al., 2009), in complexes that may include receptors such as PTH receptors. Whether such factors regulate NHE6 (or NHE1) in osteoblasts are interesting future studies. Preliminary mRNA and antibody localization studies for NHERF1 suggest that NHERF1 is expressed in some, but not all, osteoblasts (data not shown).

Ten NHE isoforms occur in mammalian cells (Slepkov et al., 2007). NHE1 is a housekeeping isoform and is widely expressed, albeit in highly variable amounts, in the plasma membranes of cells in many tissues as well as bone. NHEs 2-5 have more restricted tissue distributions, in keeping with specific transport functions such as NHE3 in the kidney and gut (Slepkov et al., 2007). NHE1 is usually basolateral, whereas NHEs 2-5 are typically expressed apically (toward the secretory surface). In this regard, the unusual expression of NHE6 at the osteoblast counter-secretory basolateral membrane may reflect the highly specialized function of the bone forming unit.

The NHE6-NHE9 isoforms typically locate in intracellular compartments (Nakamura et al. 2005), although there are precedents for NHE6 expression on cell membranes as guided by the chaperone protein RACK1 (Ohgaki et al., 2008). We confirmed that mRNA for RACK1 is present in human mineralizing osteoblasts (not shown). Other than its unusual distribution mechanism, NHE6 occurs at locations where NHE1 is also found (Hill et al., 2006; Ohgaki et al., 2008). It probably is necessary in cells requiring more specific regulation of Na^+/H^+ exchange than is possible with NHE1.

There are precedents for NHE activity in osteoblasts, including a recent report of NHE1 and NHE3 in human osteoblasts (Mobasheri et al., 1998). We cannot detect significant quantities of NHE3; however, in agreement with that report, AE2 appears to be, along with NHE1, a ‘housekeeping’ gene in osteoblasts. There are other reports of Na^+/H^+ exchange activity in osteoblasts cultures, also of non-mineralizing cells and in malignant cell lines; these older reports did not differentiate isoforms (Green et al., 1988; Redhead and Baker, 1988). We found NHE6 by restricting our analysis to cell cultures with active mineralization (Fig. 1) since NHE6 localized mainly to mineralizing bone (Fig. 5).

Our data are consistent with a model in which NHEs maintain slightly alkaline pHi in osteoblasts to promote mineralization and acid produced during mineral deposition is removed by NHEs, probably mostly NHE1 and NHE6 (Fig. 7). Because bone formation is dynamic, the proportion of actively transporting osteoblasts differs from preparation to preparation, so, while we always found very large Na^+-dependent transport, there were

minor difference between preparations in maximal acid accumulation (e.g., Fig. 2B vs. Fig. 2C). These variations do not affect the overall interpretation of the data.

In summary, our data indicate that a very high capacity of Na^+/H^+ exchange activity is involved in the maintenance of resting pHi of mineralizing osteoblasts. The transport rate dissipates strong external acid loads, either acetate or propionate, and was much higher than that found in non-mineralizing osteoblasts. Mineralizing osteoblasts maintain a slightly alkaline basal pH, probably reflecting this activity. An unusual basolateral cell surface transporter, NHE6, is likely to be a key element in this activity, although there is probably an extensive regulatory complex associated with osteoblast NHEs; this remains to be characterized. NHE1 and NHE6 may act redundantly and contribute to different mechanisms normally regulating pHi, but conditions where the two transporters have clearly divergent functions are as yet unknown. In addition, our data are consistent with HCO_3^- transport in both mineralizing and non-mineralizing osteoblasts which was not Na^+-dependent, probably reflecting AE2 expression.

Acknowledgments

This work was supported by grants from the National Institutes of Health (USA) AR053976, DK069998, and AR055208 and by the Department of Veteran's Affairs (USA).

Literature Cited

Arana-Chavez VE, Soares AM, Katchburian E. Junctions between early developing osteoblasts of rat calvaria as revealed by freeze-fracture and ultrathin section electron microscopy. Arch Histol Cytol. 1995; 58:285–292. [PubMed: 8527235]

Blair HC, Schlesinger PH, Huang CL, Zaidi M. Calcium signalling and calcium transport in bone disease. Subcell Biochem. 2007; 45:539–562. [PubMed: 18193652]

Blair HC, Yaroslavskiy BB, Robinson LJ, Mapara MY, Pangrazio A, Guo L, Chen K, Vezzoni P, Tolar J, Orchard PJ. Osteopetrosis with micro-lacunar resorption because of defective integrin organization. Lab Invest. 2009; 89:1007–1017. [PubMed: 19546854]

Brandao-Burch A, Utting JC, Orriss IR, Arnett TR. Acidosis inhibits bone formation by osteoblasts in vitro by preventing mineralization. Calcif Tissue Int. 2005; 77:167–174. [PubMed: 16075362]

Bronckers AL, Lyaruu DM, Jansen ID, Medina JF, Kellokumpu S, Hoeben KA, Gawenis LR, Oude-Elferink RP, Everts V. Localization and function of the anion exchanger Ae2 in developing teeth and orofacial bone in rodents. J Exp Zool B: Mol Dev Evol. 2009; 312B:375–387. [PubMed: 19206174]

Bustin SA. Absolute quantification of mRNA using real-time reverse transcription polymerase chain reaction assays. J Mol Endocrinol. 2000; 25:169–193. [PubMed: 11013345]

Capuano P, Bacic D, Roos M, Gisler SM, Stange G, Biber J, Kaissling B, Weinman EJ, Shenolikar S, Wagner CA, Murer H. Defective coupling of apical PTH receptors to phospholipase C prevents internalization of the Na^+-phosphate cotransporter NaPi-IIa in Nherf1-deficient mice. Am J Physiol Cell Physiol. 2007; 292:C927–C934. [PubMed: 16987995]

Cardone RA, Bellizzi A, Busco G, Weinman EJ, Dell'Aquila ME, Casavola V, Azzariti A, Mangia A, Paradiso A, Reshkin SJ. The NHERF1 PDZ2 domain regulates PKA RhoA-p38-mediated NHE1 activation and invasion in breast tumor cells. Mol Biol Cell. 2007; 18:1768–1780. [PubMed: 17332506]

Erdogan S, FitzHarris G, Tartia AP, Baltz JM. Mechanisms regulating intracellular pH are activated during growth of the mouse oocyte coincident with acquisition of meiotic competence. Dev Biol. 2005; 286:352–360. [PubMed: 16150436]

Gonçalves RR, Furriel RP, Jorge JA, Leone FA. Rat osseous plate alkaline phosphatase: Effect of neutral protease digestion on the hydrolysis of pyrophosphate and nitrophenylphosphate. Mol Cell Biochem. 2002; 241:69–79. [PubMed: 12482027]

Green J, Yamaguchi DT, Kleeman CR, Muallem S. Cytosolic pH regulation in osteoblasts: Interaction of Na^+ and H^+ with the extracellular and intracellular faces of the Na^+/H^+ exchanger. J Gen Physiol. 1988; 92:239–261. [PubMed: 2844958]

Hayashi H, Szászi K, Grinstein S. Multiple modes of regulation of Na^+/H^+ exchangers. Ann N Y Acad Sci. 2002; 976:248–258. [PubMed: 12502567]

Helbig H, Korbmacher C, Stumpff F, Coca-Prados M, Wiederholt M. Na^+/H^+ exchange regulates intracellular pH in a cell clone derived from bovine pigmented ciliary epithelium. J Cell Physiol. 1988; 137:384–389. [PubMed: 2848042]

Hill JK, Brett CL, Chyou A, Kallay LM, Sakaguchi M, Rao R, Gillespie PG. Vestibular hair bundles control pH with $(Na^+, K^+)/H^+$ exchangers NHE6 and NHE9. J Neurosci. 2006; 26:9944–9955. [PubMed: 17005858]

Kulanthaivel P, Furesz TC, Moe AJ, Smith CH, Mahesh VB, Leibach FH, Ganapathy V. Human placental syncytiotrophoblast expresses two pharmacologically distinguishable types of Na^+–H^+ exchangers, NHE-1 in the maternal-facing (brush border) membrane and NHE-2 in the fetal-facing (basal) membrane. Biochem J. 1992; 284:33–38. [PubMed: 1318024]

Miyazaki E, Sakaguchi M, Wakabayashi S, Shigekawa M, Mihara K. NHE6 protein possesses a signal peptide destined for endoplasmic reticulum membrane and localizes in secretory organelles of the cell. J Biol Chem. 2001; 276:49221–49227. [PubMed: 11641397]

Mobasheri A, Golding S, Pagakis SN, Corkey K, Pocock AE, Fermor B, O'Brien MJ, Wilkins RJ, Ellory JC, Francis MJ. Expression of cation exchanger NHE and anion exchanger AE isoforms in primary human bone-derived osteoblasts. Cell Biol Int. 1998; 22:551–562. [PubMed: 10452823]

Nakamura N, Tanaka S, Teko Y, Mitsui K, Kanazawa H. Four Na^+/H^+ exchanger isoforms are distributed to Golgi and post-Golgi compartments and are involved in organelle pH regulation. J Biol Chem. 2005; 280:1561–1572. [PubMed: 15522866]

Ohgaki R, Fukura N, Matsushita M, Mitsui K, Kanazawa H. Cell surface levels of organellar Na^+/H^+ exchanger isoform 6 are regulated by interaction with RACK1. J Biol Chem. 2008; 283:4417–4429. [PubMed: 18057008]

Okhuma S, Poole B. Fluorescence probe measurement of the intralysosomal pH in living cells and the perturbation of pH by various agents. Proc Natl Acad Sci USA. 1978; 75:3327–3331. [PubMed: 28524]

Orlowski J, Grinstein S. Diversity of the mammalian sodium/proton exchanger slc9 gene family. Pflugers Arch. 2004; 447:549–565. [PubMed: 12845533]

Prêle CM, Horton MA, Caterina P, Stenbeck G. Identification of the molecular mechanisms contributing to polarized trafficking in osteoblasts. Exp Cell Res. 2003; 282:24–34. [PubMed: 12490191]

Redhead CR, Baker PF. Control of intracellular pH in rat calvarial osteoblasts: Coexistence of both chloride–bicarbonate and sodium–hydrogen exchange. Calcif Tissue Int. 1988; 42:237–242. [PubMed: 3135089]

Roos A, Boron WF. Intracellular pH. Physiol Rev. 1981; 61:296–434. [PubMed: 7012859]

Schartum S, Nichols G Jr. Concerning pH gradients between the extracellular compartment and fluids bathing the bone mineral surface and their relation to calcium ion distribution. J Clin Invest. 1962; 41:1163–1168. [PubMed: 14498063]

Schwark JR, Jansen HW, Lang HJ, Krick W, Burckhardt G, Hropot M. S3226, a novel inhibitor of Na^+/H^+ exchanger subtype 3 in various cell types. Pflugers Arch. 1998; 436:797–800. [PubMed: 9716715]

Seidler U, Singh AK, Cinar A, Chen M, Hillesheim J, Hogema B, Riederer B. The role of the NHERF family of PDZ scaffolding proteins in the regulation of salt and water transport. Ann N Y Acad Sci. 2009; 1165:249–260. [PubMed: 19538313]

Slepkov ER, Rainey JK, Sykes BD, Fliegel L. Structural and functional analysis of the Na^+/H^+ exchanger. Biochem J. 2007; 401:623–633. [PubMed: 17209804]

Steeves CL, Lane M, Bavister BD, Phillips KP, Baltz JM. Differences in intracellular pH regulation by Na(+)/H(+) antiporter among two-cell mouse embryos derived from females of different strains. Biol Reprod. 2001; 65:14–22. [PubMed: 11420218]

Teti A, Blair HC, Teitelbaum SL, Kahn AJ, Koziol C, Konsek J, Zambonin-Zallone A, Schlesinger PH. Cytoplasmic pH regulation and chloride/bicarbonate exchange in avian osteoclasts. J Clin Invest. 1989; 83:227–233. [PubMed: 2910910]

Thomas JA, Buchsbaum RN, Zimniak A, Racker E. Intracellular pH measurement in Ehrlich ascites tumor cells utilizing spectroscopic probes generated in situ. Biochemistry. 1979; 18:2210–2218. [PubMed: 36128]

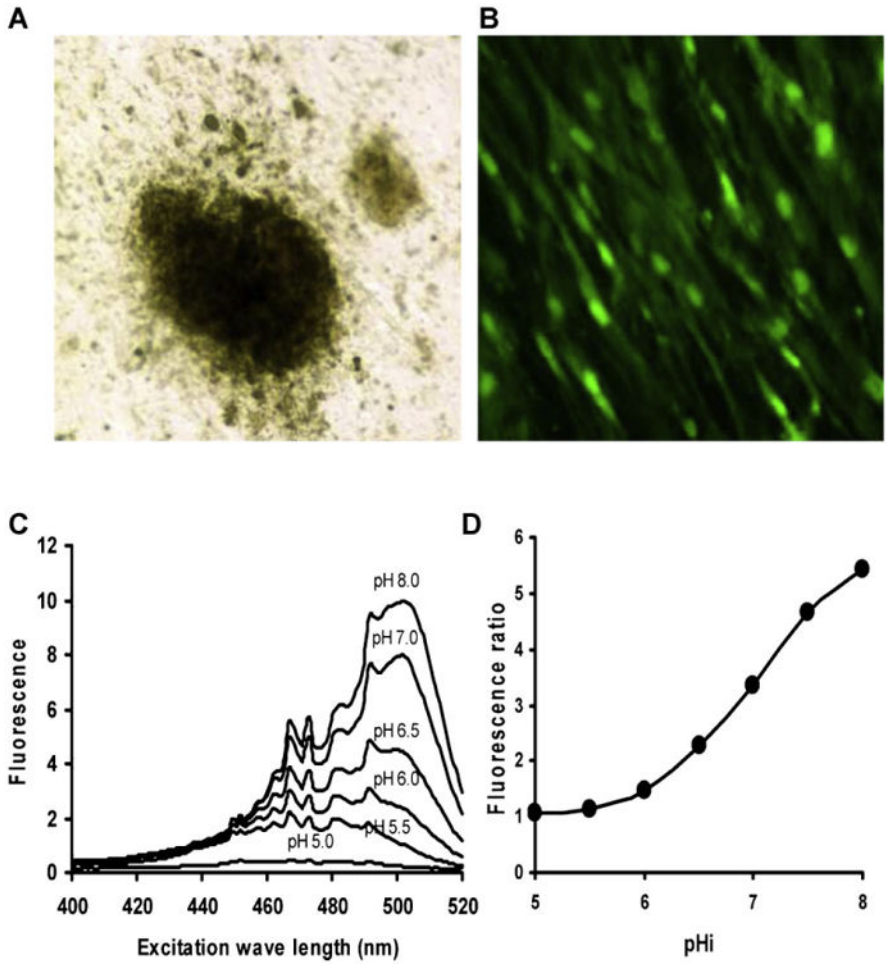

Fig. 1.

Intracellular pH measurement using 2′, 7′-bis-(2-carboxyethyl)-5, 6-carboxyfluorescein (BCECF) in non-transformed mineralizing human osteoblasts. A: Confluent normal human osteoblasts. A bright field picture without phase shows mineralization, which reflects light, as focal dark nodules. The field is 500 μm across. B: For intracellular pH measurement, osteoblasts grown and differentiated on glass chips were loaded with 5 μM BCECF-AM at 37°C for 1 h. Green fluorescence shows the intracellular loading of the dye. The field is 200 μm across. C: BCECF loaded mineralizing human osteoblasts on glass were transferred to cuvette containing 130 mM KCl, 20 mM NaCl, 5 mM Hepes, and 10 μg/ml nigericin to equilibrate intracellular and extracellular pH. Solutions were adjusted to pH 5.0, 5.5, 6.0, 6.5, 7.0, and 8.0 using NH_4OH or acetic acid. Excitation scans with excitation from 400 to 520 nm and a fixed emission at 535 nm was performed using calibration solutions at each pH level as indicated. D: A standard curves relating fluorescence ratios with background fluorescence subtracted [(F500 nm F400 nm)/(F455 nm F400 nm)] to intracellular pH, from the excitation scans (C). [Color figure can be viewed in the online issue, which is available at wileyonlinelibrary.com.]

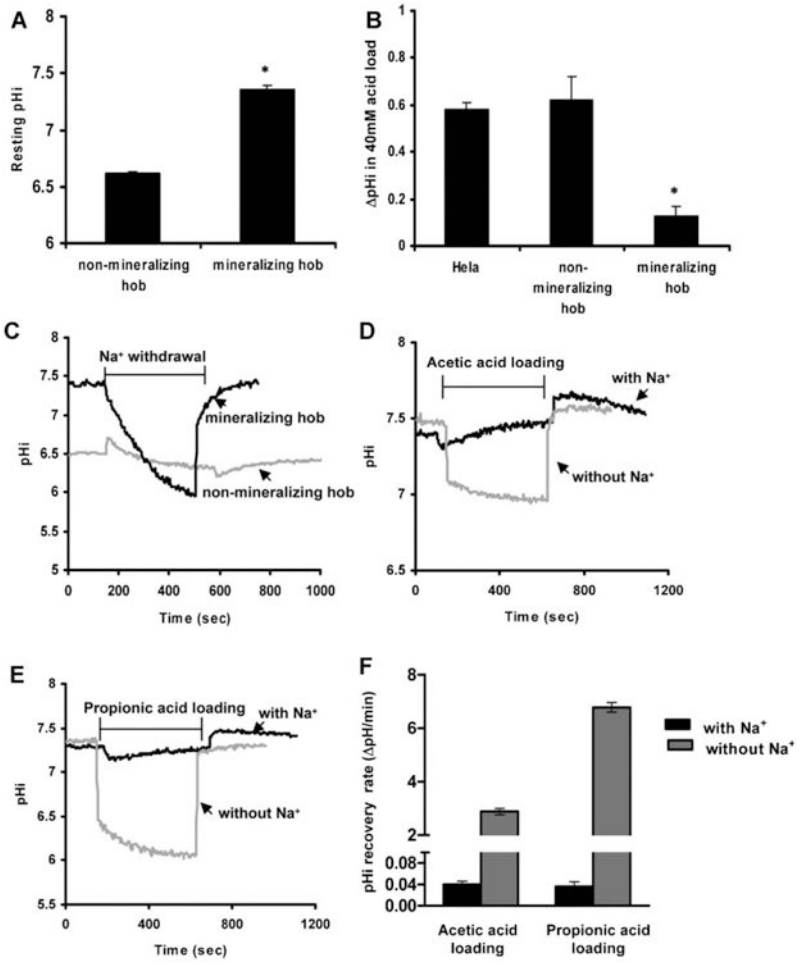

Fig. 2.

Intracellular pH changes in response to acid load and Na^+ withdrawal. BCECF loaded normal human osteoblasts or HeLacells (controls in B) were grown on glass, equilibrated in Hepes-buffered HCO_3^- free saline (standard solution): 140 mMNaCl, 3 mMKCl, 1.5 mM $CaCl_2$, 5 mM Hepes, 5 mM glucose, pH 7.4, transferred into test solutions. A: Effect of mineralization on resting osteoblast intracellular pH. Mineralizing osteoblast resting intracellular pH is significantly higher than that of non-mineralizing osteoblasts. N = 4, mean ± SD, $P < 0.01$. B: Change in intracellular pH in HeLa cells, non-mineralizing human osteoblasts, and mineralizing human osteoblasts after a 40 mM acid load using propionate acid in standard solution. The change in pH in HeLa cells and nonmineralizing osteoblasts was similar, while mineralizing osteoblasts, which express much larger amounts of sodium-hydrogen exchangers (see Fig. 4), was significantly reduced. N = 4, mean ± SD, P<0.05. C: Real-time measurements of intracellular pH: effect of replacing extracellular sodium. In mineralizing normal osteoblasts (black trace): replacement of standard solution with Na+-free solution, 140 mMN-methyl-D-glucamine chloride (NMDGCl), 5 mM Hepes, 5 mM glucose, pH 7.4from 140 to 505 sec. At 505 sec, the cells were transferred back to standard solution. Growing, non-mineralizing normal osteoblasts (grey trace): replacement of standard solution with Na^+-free solution from 150 to 580 sec. At 580 sec, the cells were

transferred backto standard solution. D: Effect of acetic acid loading on mineralizing normal human osteoblasts with and without extracellular sodium. Cells were exposed to acetic acid, 40 mM, in the presence of Na^+ (black trace), from 110 to 640 sec, then transferred back into standard solution. The same cells grown on another glass chip were exposed to acetic acid load in Na^+-free solution (grey trace) from 145 to 625 sec, then transferred back into standard solution. Standard solution with 40 mM potassium acetate was used as acetic acid load. Na^+-free acid load was the same except for the replacement of NaCl with NMDGCl. E: Effect of propionic acid loading on mineralizing normal human osteoblasts with and without extracellular sodium. Osteoblasts were exposed to propionate acid, 40 mM, in the presence of Na^+ (black trace), from 190 to 695 sec, then transferred back into standard solution. The same cells grown on another glass chip were exposed to propionate acid load in Na^+-free solution (grey trace) from 150 to 625 sec, and then transferred back into standard solution. Standard solution with 40 mM potassium propionate was used as propionate acid load. Na^+-free acid load was the same except forthe replacement of NaCl with NMDGCl. Intracellular pHwasderived asdescribed under Materials and Methods Section. F: Comparison of initial pHi recovery rate of osteoblasts from acid load in presence or absence of Na^+.

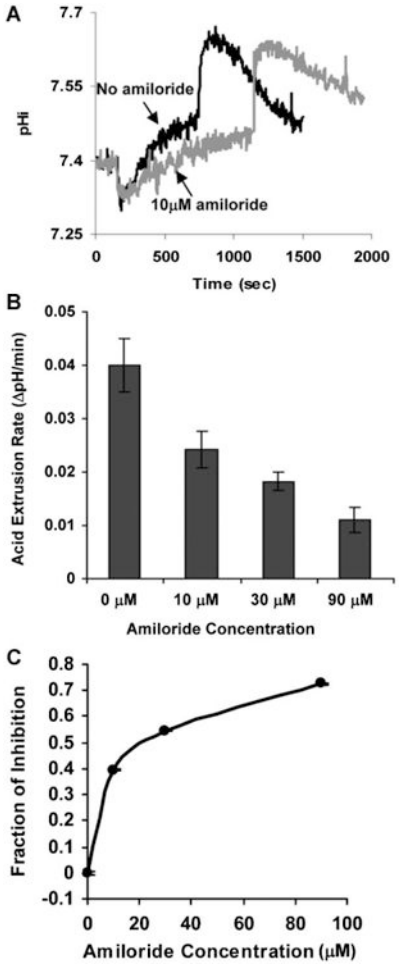

Fig. 3.

Effect of amiloride on intracellular pH recovery after acid load. A: BCECF loaded mineralizing human osteoblasts on glass were first equilibrated in 140 mM NaCl, 3 mM KCl, 1.5 mM $CaCl_2$, 5mM Hepes, 5 mM glucose, pH 7.4, and transferred into acetate loading solution in the presence (grey trace) or absence of 10 μM amiloride (black trace). For comparison the two curves are overlaid. Loading solution is standard solution plus 40 mM potassium acetate, pH 7.4. B: Acid extrusion as rate of pH recovery (in pH units/min) calculated from the initial slope of the pH recovery curves (A). N = 2, mean ± range. C: Amiloride concentration in relation to the fractional inhibition of pH recovery (B). A second independent experiment showed similar results (not illustrated).

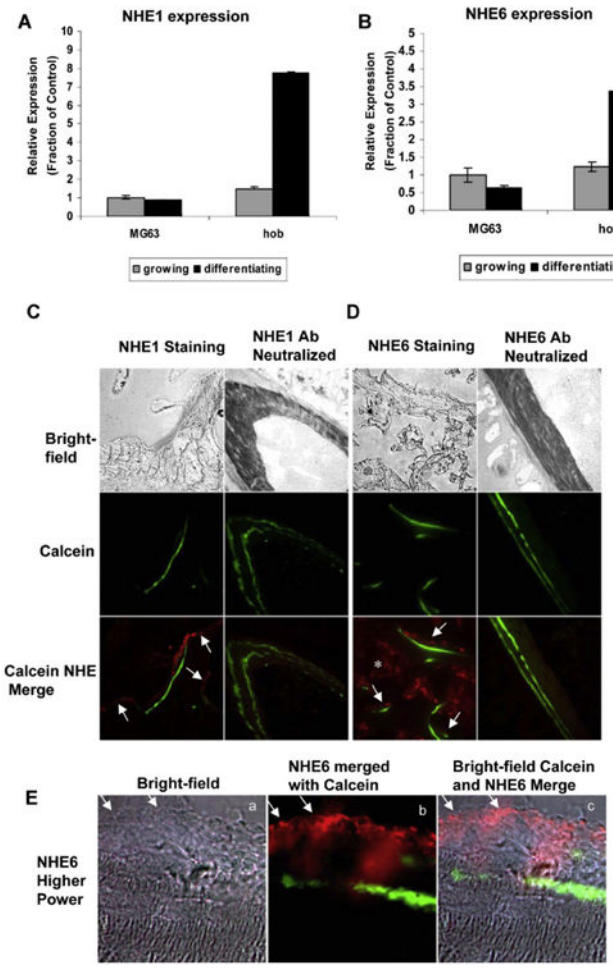

Fig. 4.

Sodium–hydrogen exchangers 1 and 6 are highly expressed in human and mouse osteoblasts. A, B: Real-time RT-PCR analysis of NHE isoform 1 (A) and isoform 6 (B) in growing and mineralizing normal human osteoblasts and MG63 human osteosarcoma cells. Total RNA were isolated from growing normal human osteoblasts and MG63cells, mineralizing normal human osteoblasts and MG63 cells treated with osteoblast differentiation medium for 2weeks. Results were presented as fraction of control. N = 2, mean W ± range. C, D: Fluorescent immune labeling of NHE 1 (C) and NHE6 (D) in mouse vertebral bone frozen sections. Sections were labeled with goat anti-NHE6, goat anti-NHE1, and secondary donkey anti-goat cy3 (red) as described in Materials and Methods Section. Negative controls using specific blocking peptide to neutralize each primary antibody are also shown (second and fourth columns). Calcein labeling of bone formation at the mineralizing surface (green signal) was shown separately (middle row) and overlaid with NHE1 orNHE6 signals (red) (last row). Bright field picture with no phase of the same field was also taken to show the contour of the bone (first row). Fields are 300 μm across. E: Labeling for calcein and NHE6 at higher magnification. Fields are 100 μm across. [Color figure can be viewed in the online issue, which is available at wileyonlinelibrary.com.]

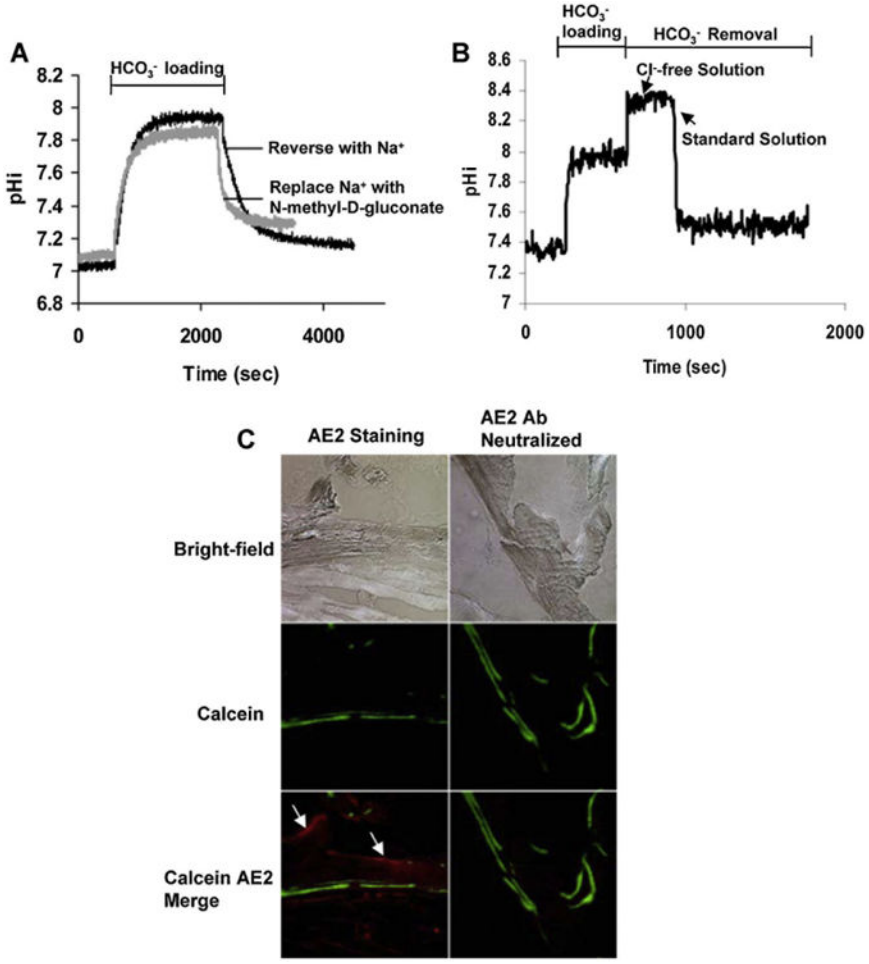

Fig. 5.

HCO_3^-/Cl^- exchange activity and anion exchanger 2(AE2) in osteoblasts. A: BCECF loaded mineralizing human osteoblasts grown on glass first equilibrated in standard solution, 140 mM NaCl, 3 mM KCl, 1.5 mM $CaCl_2$, 5 mMHepes, 5 mM glucose, pH 7.4, and transferred into bicarbonate loading solution: 40 mM $NaHCO_3$, 100 mM NaCl, 5 mM Hepes, 5 mM glucose, pH 7.4. The base loading was reversed by transferring the cells into standard solution (black curve) or Na^+-free solution with Na^+ replaced with N-methyl-D-glucamine ($NMDG^+$) (grey curve). Intracellular pH was derived as described in Materials and Methods Section. B: Bicarbonate-loaded cells as in A were transferred into bicarbonate free medium but with chloride replaced with gluconate; pHi did not re-equilibrate until this Cl^- free solution was additionally replaced with standard chloride-containing medium. C: Indirect fluorescent labeling of antibody localization of AE2 in mouse vertebra frozen sections. Sections were cut and labeled with goat anti-AE2 and donkey anti-goat-Cy3 (red) as described in Materials and Methods Section. Negative controls using AE2 specific blocking peptide to neutralize primary AE2 antibody are shown (right column). Calcein labeling of bone formation at the mineralizing surface (green signal) was shown separately (middle row) and overlaid with AE2 signal (red signal) (last row). Note that the basolateral surface of bone lining cells, with or without calcein (green signal), is labeled with the

antibody. Bright field of the same area is shown to indicate the contour of bone trabeculae (first row). All fields shown are 300 μm across. [Color figure can be viewed in the online issue, which is available at wileyonlinelibrary.com.]

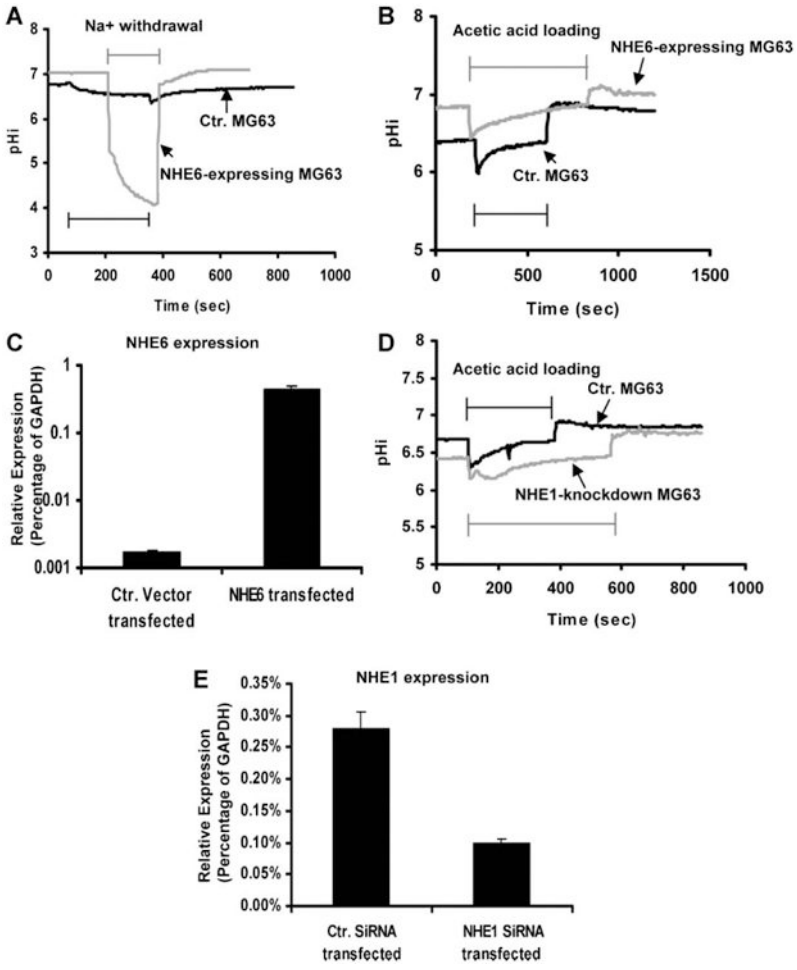

Fig. 6.

Effect on pHi of overexpression of NHE6 or NHE1 knockdown in MG63 cells. MG63 cells grown on glass were transfected with either control vector, NHE6-expressing plasmid, control siRNA, or NHE1 siRNA. Forty-eight hours later, a glass chip was loaded with BCECF and equilibrated in standard solution. Standard solution, Na^+-free solution, and acetic acid load solution are the same as in previous figures. A: Effect of NHE6 over expression on Na^+ withdrawal in MG63 cells. Black trace: control vector transfected MG63 cells were exposed to Na^+-free solution from 90 to 355 sec then transferred back into standard solution. Grey trace: MG63 cells transfected with NHE6-expressing plasmids were exposed to Na^+-free solution from 210 to 380 sec then transferred back in to standard solution. Horizontal bars indicate periods of Na^+ withdrawal. B: Effect of NHE6 over expression on acetic acid load in MG63 cells. Black trace: control vector transfected MG63 cells were exposed to acetic acid loads olution from 210 to 610 sec then transferred back in to standard solution. Grey trace: MG63 cells transfected with NHE6-expressing plasmids were exposed to acetic acid load from 185to 835 sec then transferred back into standard solution. Horizontal bars indicate periods of acetic acid loading. C: Real-time PCR analysis of NHE6 expression in MG63 cells transfected with control vector or NHE6-expressing plasmid. Results are presented as percentage of GAPDH level. Note that the difference is several hundred fold; the Y-axis is log scale. D: Effect of NHE1 knockdown on acetic acid

load in MG63 cells. Black trace: control siRNA transfected MG63 cells were exposed to acetic acid load solution from 105 to 380 sec then transferred back into standard solution. Grey trace: MG63 cells transfected with NHE6-expressing plasmids were exposed to acetic acid load from 105 to 565 sec then transferred back into standard solution. Horizontal bars indicate periods of acetic acid loading. E: Real-time PCR analysis of NHE1 expression in MG63 cells transfected with control siRNA or NHE1 siRNA. Results are presented as percentage of GAPDH level.

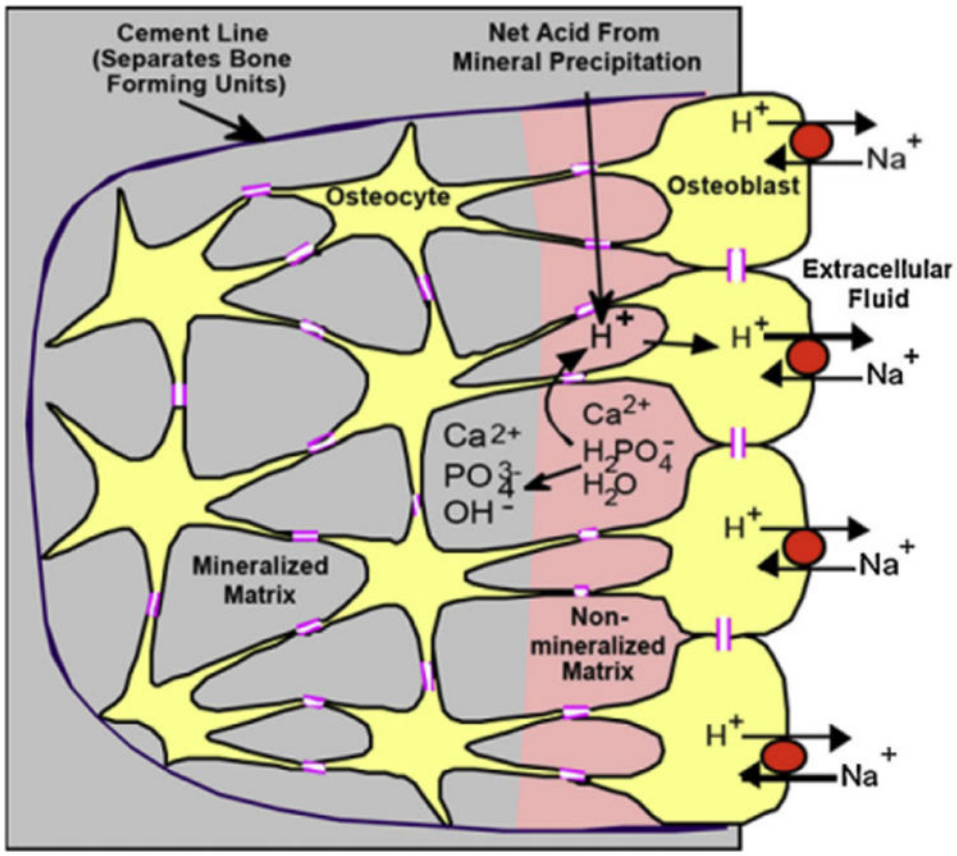

Fig. 7.

Proposed sodium-hydrogen exchange mechanism to alkalinize the bone mineral formation compartment, which produces net acid. Bone is formed by gap-junction linked groups of osteoblasts, this unit referred to as an osteon. Its superficial (bone lining) cells isolate extracellular fluid from the bone matrix with tight junctions. Its deep surface is a cement line; mineralized bone is deposited from the cement line toward the surface at a narrow front. As cells are incorporated in matrix, new layers of osteoblasts differentiate at the basolateral surface and are added to the unit. Cells buried in matrix no longer synthesize bone, but have regulatory functions, and are called osteocytes. Mineralized bone is impervious to ions, so deposition of mineral is strictly vectorial. At the mineralization front, $H_2PO_4^-$ and water are precipitated with Ca^{2+} as a PO_4^{3-} and OH^- salt, with evolution of H^+, ~1.5 moles per mole of Ca^{2+} deposited. The osteoblasts maintain a slightly alkaline pH, which promotes mineral precipitation, and manage the acid produced, by greatly expanded expression and activity of sodium-hydrogen exchangers NHE1 and NHE6 at their basolateral surfaces. [Color figure can be viewed in the online issue, which is available at wileyonlinelibrary.com.]